Integrated Electronics for a Reading Aid for the Blind

J. S. BRUGLER, MEMBER, IEEE, JAMES D. MEINDL, FELLOW, IEEE, JAMES D. PLUMMER, PHILLIP J. SALSBURY, MEMBER, IEEE, AND WILLIAM T. YOUNG

Abstract—**A novel direct-translation reading aid for the blind has been developed using integrated electronics. Image sensing is accomplished by a 144-element monolithic phototransistor array. Photo signals are processed by efficient multiplex circuitry, with automatic compensation for optical changes in reading material. A tactile output image is provided by an array of vibratory piezoelectric reeds. Encouraging test results indicate that the reading aid could become widely used among the blind.**

I. Introduction

INTEGRATED electronics has made feasible a multitude of low-cost, small-size, high-performance implements not possible in the past. In particular, relatively sophisticated personal electronic aids for the handicapped that have been envisioned for some time may now be realized. Among these is the reading aid described in this paper, which combines a basically old idea with modern technology to achieve a novel result. In essence, the result is a practical self-contained reading instrument, which allows a blind person immediate access to virtually all printed material used by sighted people. The instrument is designed to eliminate the "middle man" presently required for converting printed matter to braille or speech output. Integrated electronics is of crucial importance to this goal.

A number of reading aids have been previously built, but none has become widely used. Most of these devices [1]–[3] use an auditory output, following the pioneering work of Fournier d'Albe [4]. A common deficiency of these machines has been inadequate resolution [5], i.e., too few photocells to unambiguously identify all input patterns. Consequently, maximum reading rate with most subjects has been less than ten words per minute. In addition the single audio channel available seems less well suited to letter pattern identification than the parallel processing of the tactile sense. The aforementioned difficulties are surmounted in the present device by use of an integrated photosensor, multiplexing electronics, and a multichannel tactile output. The perceptual foundations of the aid are considered in [5] and [6]. The optoelectronic design is of chief interest in the present paper.

The direct-translation principle of operation is employed, as detailed in earlier publications [7], [8]. The system design is based on computer-controlled reading tests and a continuing hardware evaluation program, both using blind subjects. Both hands are used for operation, as shown in Fig. 1. One hand holds the reading probe, and by scanning it across the printed page causes a moving tactile image to be presented to the index finger of the opposite hand. This tactile image is a direct reproduction of the printed material, taken approximately one letter at a time. Reading is accomplished by tactile recognition of the letter patterns that move, under user control, beneath the finger. In the present model a 24 × 6 monolithic phototransistor imaging array is connected, via multiplex electronics, to a corresponding 24 × 6 output array of vibratory piezoelectric reeds or bimorphs.[1] Each bimorph contacts the skin via a nickel pin protruding through a small hole in a perforated plastic plate. A bimorph vibrates if the illumination on its re-

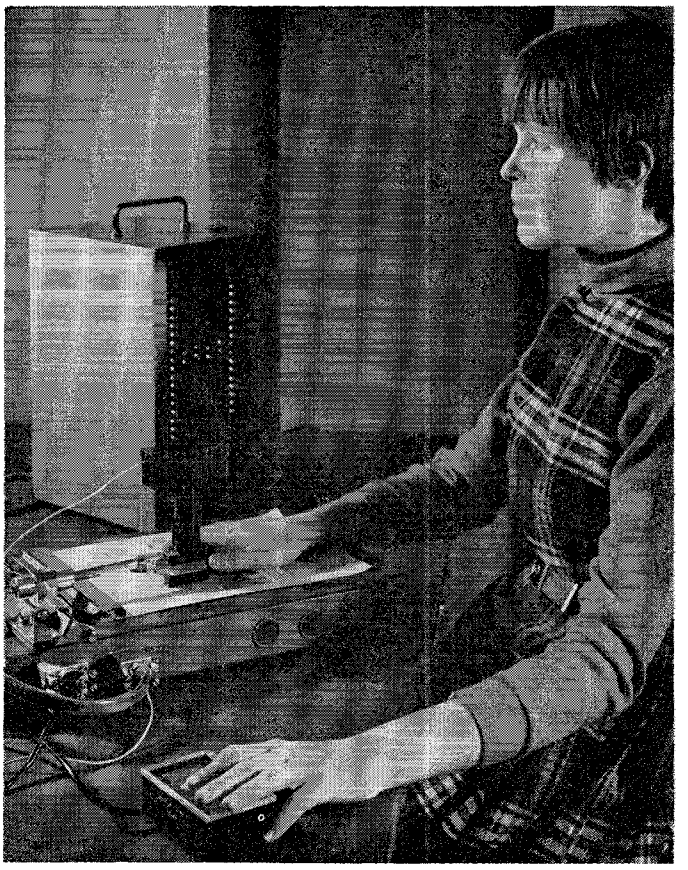

Fig. 1. Reading aid showing probe guided by right hand of operator, electronics beneath tracking aid, and light box.

Manuscript received April 11, 1969; revised June 13, 1969. This work was supported by a grant from the U. S. Office of Education, Department of Health, Education, and Welfare. However, the opinions expressed herein do not necessarily reflect the position or policy of the U. S. Office of Education, and no official endorsement by the U. S. Office of Education should be inferred.

The authors are with the Department of Electrical Engineering, Stanford University, Stanford, Calif. 94305.

[1] "Bimorph" is a trade name of the Clevite Corporation.

spective phototransistor falls below a preset threshold. The resultant image is thus quantized in both space and intensity. For the benefit of a sighted observer, the image can be displayed on a light box as shown in Fig. 1.

II. The Optoelectronic Design

Fig. 2 presents a simplified system block diagram [9]. Each letter is focused by a simple lens system onto the phototransistor array. This monolithic array consists of six columns of 24 transistors, operated in the charge storage, or integration mode. The asymmetry of the 24 × 6 arrangement is exploited through use of one-dimensional "*y*" multiplexing. A 24-stage shift register performs this function. The six signal channels drive six comparators, which accomplish light–dark signal quantization. The comparator and shift register signals comprise x and y inputs to a 24 × 6 transistor array, connected one-for-one to the tactile output stimulators. The bipolar transistor array simultaneously decodes the multiplexed information and energizes the appropriate bimorphs. Although with this scheme, each piezoelectric reed is driven at a very low duty cycle, its self-capacitance provides adequate temporary memory for satisfactory operation. The system frame rate, 200 Hz, is the resonant frequency of the stimulators. An automatic threshold control circuit (ATC) is incorporated in the system to automatically set the light–dark comparator threshold in response to different page illuminations and reflectivities. Primary electrical power is supplied by rechargable batteries, imposing a low-power drain constraint on the system design.

The monolithic phototransistor array [10], [11] used in the reading aid is a custom device designed and fabricated in the Integrated Circuit Laboratory at Stanford University. The remainder of the electronics is composed of commercial integrated circuits and discrete devices. However, adaptability has been maintained for increased levels of integration with special-purpose circuits to reduce cost and improve performance.

A. Reading Unit

The "eye" of the reading aid is the hand-held probe scanned across the printed page by the operator. A conventional optical design, illustrated in Fig. 3, is presently used. The letter space is illuminated by two incandescent bulbs. The reflected light is filtered and focused with a simple lens system onto the phototransistor array. Presently a fixed magnification is used, with the anticipation of incorporating a variable magnification in future designs. The probe contacts the page with two rollers, so that it moves easily across the page. A mechanical tracking aid (see Fig. 1) is used as a training aid to facilitate scanning along the line of print. The tracking aid constrains the probe to horizontal movement, unless a lever is pushed to release a vertical locking mechanism.

Small size plus light weight are prerequisites for an easily manipulated hand-held probe. A low lens magnification is desirable from both the standpoint of minimizing overall probe length and of minimizing required light-bulb illumination. Unity magnification is employed, making the image size too small for discrete photodevices to be conveniently utilized. The monolithic photoarray is therefore very attractive, particularly since the required number of elements is small enough for good yield. Other advantages of a monolithic structure are good matching of the photo response from element to element and precise geometrical structure. Also, the required scan rates are relatively slow, so that switching transients are not too troublesome. Fig. 4 slows a photomicrograph of the entire array. The element spacing (5 mils) in the "*y*" axis is chosen to achieve high enough spatial sampling rate for unambiguous resolution of pica type [5]. Twenty-four elements per column are used in order to adequately span the letter height. The number of columns is based on psychological considerations. Reading experiments [5] have shown marked improvement in reading performance as the number of columns is increased, so six columns are used in the present device. The columns are spaced 10 mils apart, and successive columns are displaced 2.5 mils vertically. The column staggering gives an interlaced scan effect that increases resolution.

The array has been fabricated with conventional 5-mask bipolar technology. The parameters of the phototransistors of the array have been tailored for the reading-aid application. Advantage is taken of the 24 × 6

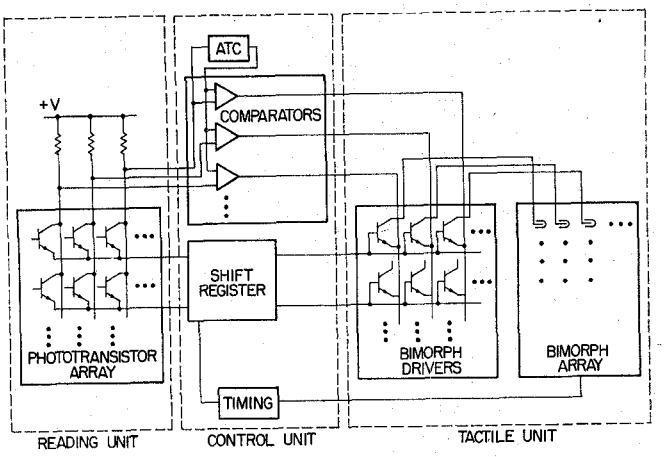

Fig. 2. Simplified system block diagram.

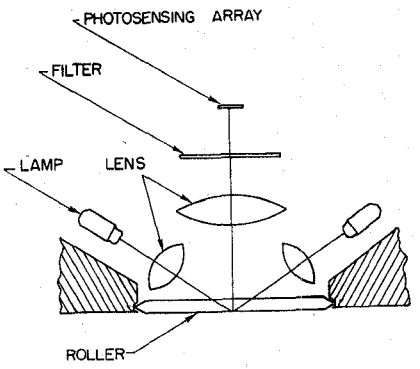

Fig. 3. Probe optomechanical design.

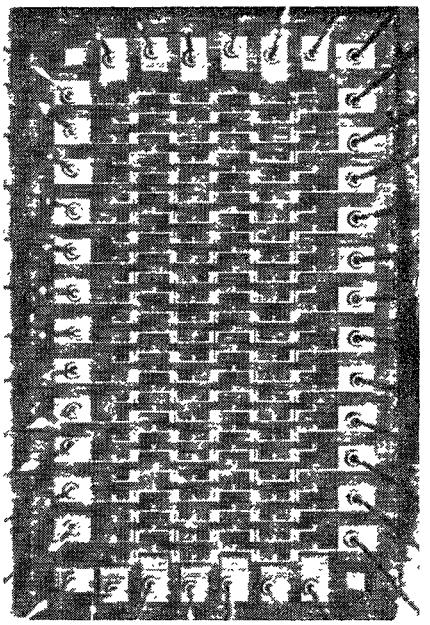

Fig. 4. Photomicrograph of sensor array.

array asymmetry by isolating each column in a common-collector island. The one-dimensional "y" multiplexing system gives simultaneous readout of each row in six parallel signal channels. The charge-storage or integration mode [12]–[14] of phototransistor operation is employed. In this particular charge-storage configuration, the signals are extracted from the transistor–collectors by 50-μs negative sampling pulses applied to their emitters. Between sampling pulses, charge is liberated at the collector–base junction by the incoming radiation. This charge, multiplied by the phototransistor h_{FE}, is delivered to the load during the sampling time. A first approximation of the output voltage waveform is an exponential pulse;

$$v_o(t) = \frac{I_P T_i}{C_{TC}} e^{-t/h_{FE}R_L C_{TC}} \tag{1}$$

where

I_P collector–base photocurrent
C_{TC} collector–base-junction capacitance
T_i charge integration time
h_{FE} phototransistor dc current gain
R_L load resistor.

The peak output voltage equals the change in voltage across the collector–base junction during the integration time, and is independent of the phototransistor current gain. For this reason, peak voltage comparators are employed in the processing circuitry. An additional feature, not available in most solid-state image sensors, is that sufficient gain is provided by each phototransistor such that no additional amplification is required prior to the comparators.

Fig. 5 is a schematic drawing of a 2 × 2 section of the array and associated waveforms. The upper-left and lower-right transistors are taken to be illuminated. Interrogation pulses are applied to the common-emitter rows, signals are extracted from the common-collector columns, and the bases are open. The load resistances, 20 kΩ, are chosen for a 10-μs output time constant so that the output pulse transient $v_o(t)$ has essentially vanished by the end of the sample time. This eliminates "memory" of the output from one cycle to the next that degrades transient response. Fig. 6 is an oscillogram showing the 24 outputs from one column of a uniformly illuminated array. The upper trace, taken with 1-volt peaks, shows good ±9 percent uniformity. The lower trace is taken at 0.1-volt peaks, and the uniformity is degraded to ±15 percent. The loss of uniformity with reduced signal level is generally observed. It is mainly due to increased sensitivity of output to various array parameters as a result of the influence of the emitter–base junction characteristic. This effect is not shown by (1), but appears in the following more accurate equation relating peak output voltage to photocurrent:

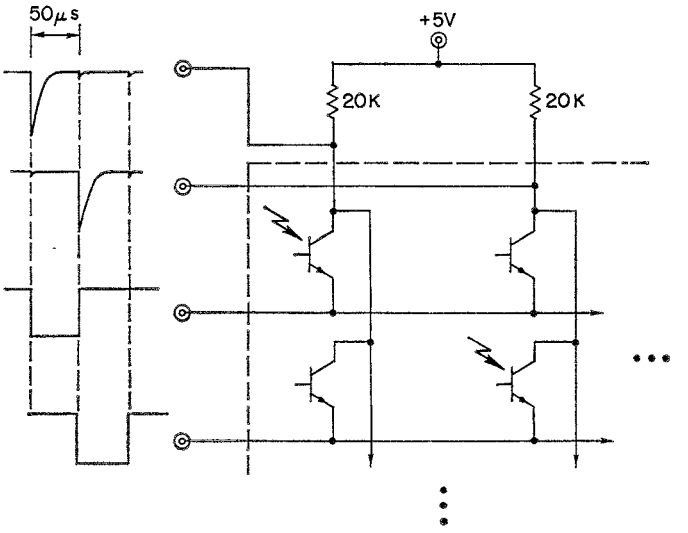

Fig. 5. Phototransistor multiplexing scheme.

$$V_P\left(1 + \frac{C_L}{h_{FE}C_{TC}}\right) + \frac{kT}{q} \ln\left(\frac{V_P}{h_{FE}R_L I_P}\right) = \frac{I_P T_i}{C_{TC}} \tag{2}$$

where

V_P peak output voltage
C_L load capacitance.

Using (2), the sensitivity of V_P to h_{FE} variations is readily derived:

$$\frac{dV_P}{dh_{FE}} \frac{h_{FE}}{V_P} = \frac{1 + \left(\frac{V_P}{kT/q}\right)\left(\frac{C_L}{h_{FE}C_{TC}}\right)}{1 + \left(\frac{V_P}{kT/q}\right)\left(1 + \frac{C_L}{h_{FE}C_{TC}}\right)}$$

$$\cong 0 \qquad V_P \gg kT/q, \quad h_{FE}C_{TC} \gg C_L. \tag{3}$$

The above shows that if the peak output voltage is to be independent of h_{FE}, V_P must be much greater than kT/q, and $h_{FE}C_{TC}$ must be much greater than C_L.

Fig. 5 shows that, even in the absence of illumination, a transient output appears. This is direct feedthrough of

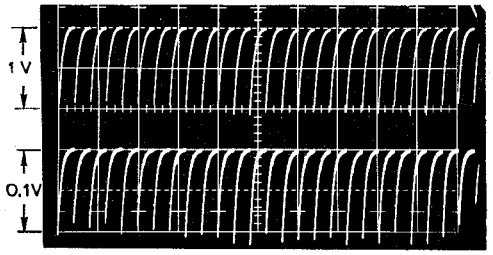

Fig. 6. Phototransistor signals from one column at 1- and 0.1-volt peak outputs.

the sampling pulse via the transistor emitter–collector capacitance. Fortunately, this feedthrough pulse has no first-order effect on the output natural mode of (1). Its magnitude is reduced by load capacitance, hence it is desirable to maintain the inequality $C_L/C_{TE} \gg 1$ to reduce feedthrough. Analysis [11] has shown that, at high-signal levels, emitter capacitance can also precipitate a "sneak-path" effect within a column whereby the output signal from an illuminated transistor drives a neighboring device into its inverse mode of operation. This effect leads to spurious output signals, and must be avoided to maintain highest image fidelity. Fortunately, the effect can be eliminated over any given range of output levels by proper choice of the ratio C_{TC}/C_{TE} For this application, normal operation is insured by maintaining $C_{TC}/C_{TE} \geq 5$.

The preceding brief discussion of array circuit considerations may be summarized as follows.

1) Sufficient illumination must be provided so that $V_P/(kT/q) \gg 1$, say V_P at least 0.25 volt.
2) The inequalities $h_{FE}C_{TC} \gg 1$, $C_L/C_{TE} \gg 1$, and $C_{TC}/C_{TE} \geq 5$ must be maintained.

The capacitance inequalities hold only if h_{FE} is large; hence, the phototransistors are designed for $h_{FE} \geq 100$ at 1-μA collector current.

Fig. 7 shows a photomicrograph of an array phototransistor. The base area is 100 × 180 μm and the emitter is 30 × 30 μm. Approximately $\frac{6}{10}$ of the cell area is photosensing. Only the emitter metalization is visible, the collectors being contacted at the array extremities. Approximate values of the various capacities are C_{TE} = 1 pF, C_{TC} = 5.5 pF, and C_L = 40 pF, where C_L is primarily the junction capacitance from collector to substrate. With h_{FE} = 100, the inequalities described above are satisfied.

The spectral response of the array is important if good performance is to be maintained with various types and colors of print. Certain dye inks, for example, have poor contrast in the near infrared, although appearing sharp to the eye. It seems reasonable, since print is optimized for sighted readers, that the spectral response of the probe should approximate that of the human eye. The vertical geometry of the array is therefore structured to maximize visible and minimize NIR photoresponse. The passivating oxide thickness (0.47 or 0.65 μm) is chosen for best antireflection properties at λ = 0.56 μm.

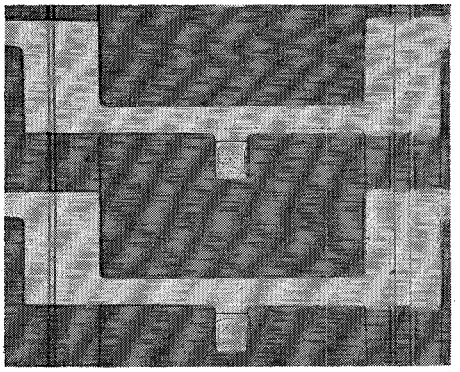

Fig. 7. Single array phototransistor cell.

Low surface recombination and a 2-μm base–collector junction depth give high device quantum efficiency at visible wavelengths. The 10-μm collector–substrate junction helps reduce NIR response by collecting all carriers liberated in its vicinity [15]. The external filter must, however, be added to sharply attenuate sensor response at wavelengths longer than 0.6-μm. The relative spectral response of the phototransistor-filter combination is depicted in Fig. 8.

Since a low-power design is required, it is of interest to compute the required page illumination. Because the spectral response peaks in the visible, a single wavelength computation at λ = 0.56 μm is appropriate. The photocurrent is

$$I_P = \eta_p \lambda A_p E_{pe}/1.24 \tag{4}$$

where

1.24 = $hc/q(V \cdot \mu m)$
η_p quantum efficiency, 0.6
λ wavelength, 0.56 μm
A_p base photodiode area, 1.8 × 10^{-4} cm^2
E_{pe} irradiance, W/cm^2.

Using (1), the peak output voltage is

$$V_P = \frac{\eta_p \lambda A_p E_{pe} T_i}{1.24 C_{TC}}.$$

Substituting appropriate values, and assuming a 0.25-volt peak voltage is desired, one finds $E_{pe} \cong 6\mu$W/cm^2, or about 4 fc. Considerably more page illumination is required because of the effect of the lens. Page irradiance E_{ie} and array irradiance E_{pe} are related by the formula

$$E_{pe} = \rho t (\mathrm{NA})^2 E_{ie} \tag{5}$$

where

ρ page reflectance, ~0.8 (white)
t lens transmission, ~0.9
NA lens numerical aperture, ~0.15.

Using (5) one finds 360 μW/cm^2 or 240 fc is necessary on the page to achieve 0.25-volt signal peaks from the array.

To compute the necessary lamp power, the following formula may be used:

$$E_{ie} = \frac{P_{in}\eta_l \eta_i}{144 A_c} \tag{6}$$

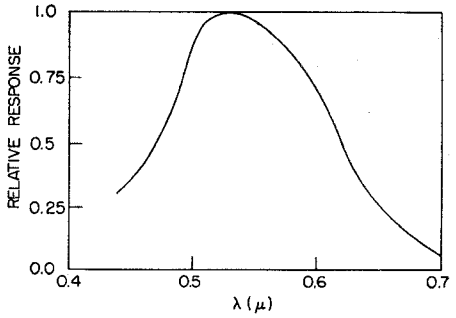

Fig. 8. Relative response, phototransistor plus 4-97 filter.

where

E_{ip} required page illuminance, 240 fc
P_{in} lamp input power, watts
η_l lamp luminous efficiency, $\sim$ 3 lm/W
η_i efficiency of page illumination
A_c unit cell area.

The quantity $P_{in}\eta_l/144A_c$ is the page illuminance if all of the lamp luminous flux were concentrated on the array; the factor η_i accounts for the losses in the actual illumination optics. Substituting appropriate values:

$$P_{in} \cong \frac{4\text{mW}}{\eta_i}. \tag{7}$$

In the present system, using a simple lens-end bulb scheme, η_i is about 0.4 percent, so the required lamp power is 1 watt. It is hoped that more-efficient optics will reduce this power substantially.

B. Tactile Unit

The tactile output unit, using vibratory reeds, is a unique system component. Considerable user experience has proven the suitability of the piezoelectric stimulator array for the reading aid. Mechanical vibration was chosen from the various possibilities for tactile stimuli because a painless sensation is obtained with good two-point discrimination. Also, the bimorphs are simple and convenient, and consume little power. Fig. 9 shows the cantilevered bimorph arrangement employed. Each bimorph, having dimensions 0.02 × 0.04 × 1.5 inches, is expoxied to an aluminum base, and extends 1.3 inches beyond its support. A 10-mil-diameter nickel pin is attached with a suitable adhesive to the bimorph tip. This pin protrudes through a 0.04-inch-diameter hole in a plastic plate whence it contacts the finger. The bimorph consists of two slabs of piezoelectric ceramic sandwiched between conducting electrodes. It operates in a mechanical push–pull fashion. Upon application of a voltage, the differential motion of the top and bottom piezoelectric slabs causes flexure of the bimorph. Electrical connection is made with magnet wire soldered to the electrodes. Both "parallel-" and "series-" poled bimorphs are available, i.e., the two halves of the bimorph sandwich are connected either in parallel or in series for proper operation. Parallel units have been used thus far, but series units will be used in the future since fewer

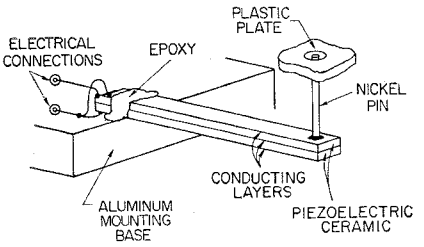

Fig. 9. Individual piezoelectric stimulator.

electrical connections are required. In operation, ac excitation is applied at the mechanical resonance frequency of the cantilever structure, 200 Hz, and, when unloaded, the peak-to-peak excursion of the bimorph tip is about 60 mils. The excursion is reduced to about 10 mils by the finger load.

The photograph, Fig. 10, shows the assembled 24 × 6 stimulator array. The three left-hand columns of pins are driven by three tiers of 24 bimorphs assembled as described above. The three right-hand columns are similarly driven in a symmetrical fashion. Only the top tiers, which drive the outside columns, are easily seen in the photograph. The same 2:1 aspect ratio and staggered columns of the sensor array are maintained. The column spacing is approximately 0.1 inch and row spacing 0.5 inch, to give an overall size of 0.5 × 1.2 inch—about 100 times the area of the phototransistor array. The perforated plastic plate is tailored to fit the curvature of the finger.

The Q of the bimorph resonance is about 20, which is a good compromise value. Too high a Q would cause array uniformity difficulties and slow transient response, while too low a Q would result in small pin deflections. It is fortuitous that the 200-Hz resonant frequency is nearly optimum with respect to the tactile sense [5]. The electrical input impedance[2] [7] of the bimorph is primarily capacitive. This self-capacitance ($\sim$0.01 μF for the parallel-poled units) is used to advantage in the system to accomplish temporary storage. In previous system realizations [8], a flip-flop was required for this purpose. A storage element is needed because the charge-storage phototransistors only provide information to each channel for a small fraction of the system frame time. The bimorph responds primarily to the harmonic of the drive signal nearest its resonant frequency. With a low-duty-cycle drive, this harmonic is quite small, so the bimorph responds weakly. This difficulty can be overcome by the series–parallel switch scheme illustrated in Fig. 11(a). The bimorph capacity is charged by the series switch that is closed during an element sample time. A half cycle later the parallel switch is briefly closed in order to discharge the bimorph. This technique enables the bimorph to be energized with an approximation to a square waveform, in spite of a low-duty-cycle switch drive. The

[2] The bimorph stimulators exhibit significant nonlinearities, both with respect to amplitude and load changes, which are disregarded in this discussion.

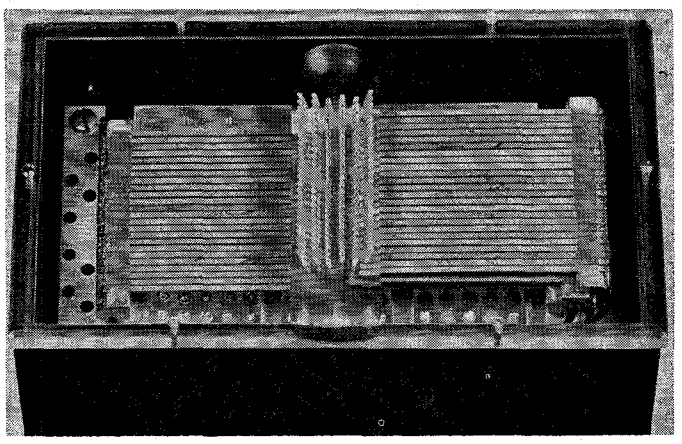

Fig. 10. Tactile stimulation array.

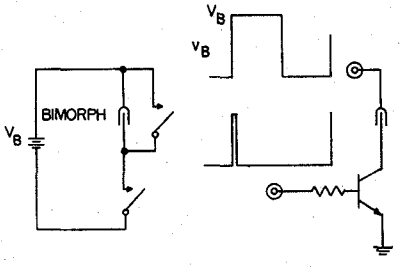

Fig. 11. Bimorph drive circuits. (a) Two-switch equivalent. (b) Actual circuit.

circuit shown in Fig. 11(a) has the disadvantage of requiring two switches at each bimorph, so the circuit of Fig. 11(b) is actually used. A square wave V_B is applied to one end of the bimorph, while the other is driven by a transistor switch. If the bimorph is to be energized, the switch is saturated during an element sample time, charging the bimorph capacitor to V_B. When V_B is returned to ground, the bimorph capacitance is discharged through the collector–base diode of the switch transistor.

Fig. 12 shows how the bimorph drive scheme is extended to the multiplex array situation. It is most convenient for one side of all the bimorphs to be common. An asymmetrical square wave is applied to this common point. In order to achieve adequate drive to all of the bimorphs, each must be charged shortly following the leading edge of the square wave, since all are discharged simultaneously at the trailing edge of the square wave. The desired "y" or row multiplexing must therefore be done during a time much smaller than the 5-ms frame time. The element sample time chosen is 50 μs, so all 24 rows are multiplexed in 1.2 ms. As shown on the figure, the first row is pulsed immediately after the leading edge of the common square wave, and 24th row 1.15 ms later. Because of the delay between the charging of the first row of bimorphs and the 24th row, the duty cycle of the bimorph drive voltage varies from top to bottom of the array. The timing is arranged so that the duty cycle varies symmetrically with respect to $\frac{1}{2}$. Since the first harmonic of a square wave varies as sin (πd), where d is the duty cycle, it varies slowly with d near $\frac{1}{2}$. The bimorph vibration amplitude therefore varies insignificantly ($\pm$ 3 percent) from top to bottom of the array. Another important feature to be noted is that the switch transistor performs the AND function necessary to demodulate the multiplexed comparator signals, thereby determing whether each bimorph is to be energized. The emitters in each column are common. If an emitter is high when the base drive signal is applied, the transistor remains off, and the bimorph is not energized. Conversely, the transistor is turned on and the bimorph excited if an emitter is low. If two-dimensional multiplexing were used, a more difficult three-input AND function would be required to gate the comparator signals.

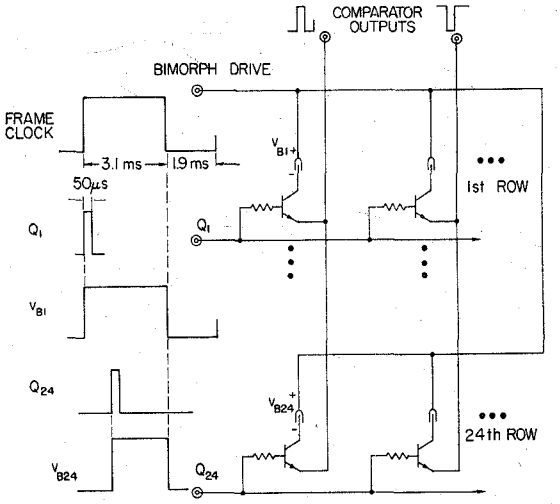

Fig. 12. Stimulator array drive circuitry.

The power necessary to drive the stimulator array is readily calculated, being almost all dissipated in the charging and discharging of the bimorph capacitance. With reference to Fig. 11(a), the charge $Q = CV_B$ is drawn every frame time T_t from the battery, for an average current drawn CV_B/T_t. The power drawn is

$$P_{\text{bimorph}} = \frac{CV_B^2}{T_t}. \tag{8}$$

The above formula holds also for the array of Fig. 12. Using

C = 0.01 μF (parallel poled)
V_B = 30 volts
T_t = 5 ms,

the worst-case power drawn by 144 bimorphs is 0.26 watt. The average power drawn is much less, since only a small fraction of a printed page is inked.

The light-box output display seen in Fig. 1 deserves brief mention. It receives the same multiplex signals as the bimorph drives, and, using a similar gating scheme, displays the tactile pattern on an array of neon bulbs. This is, of course, for the sole benefit of a sighted observer or experimenter.

C. The Control Circuitry

The control circuity performs the requisite system timing and signal processing functions between the input

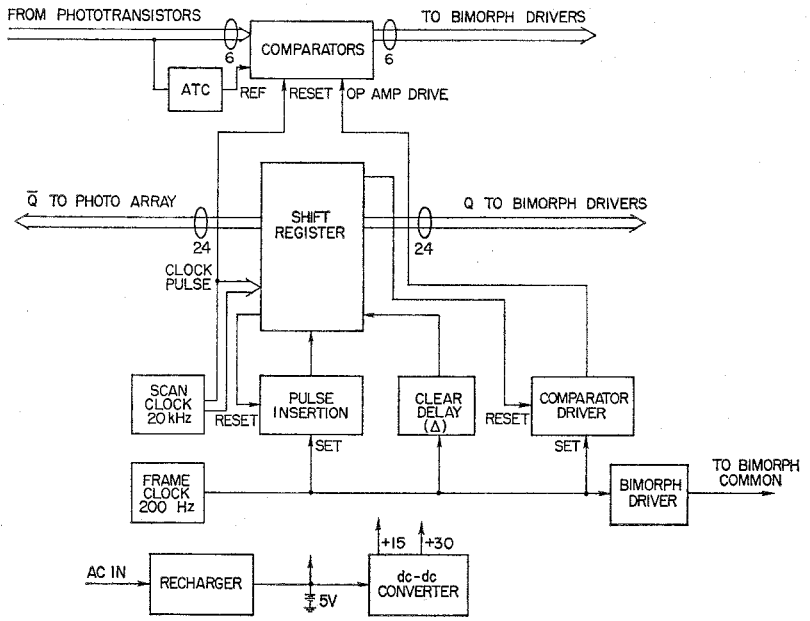

Fig. 13. Control electronics block diagram.

and output units. Fig. 13 is a functional block diagram of these electronics.

The timing is complicated somewhat by two factors: 1) the necessity for scanning the array in about one-fourth the frame time for proper stimulator drive, as described above, and 2) the necessity for a low-power design. The second requirement affects the timing through the use of pulsed, rather than continuously energized comparators. This power-saving technique is utilized since inexpensive, fast, low-power comparators are not readily available.

A two-clock scheme is used. The frame clock supplies the asymmetrical 200-Hz square wave that powers the stimulators. The scan clock, not synchronized with respect to the frame clock, furnishes the 20-kHz clock pulse drive to the shift register. The $\bar{Q}$ outputs of the 24-stage shift register scan the phototransistor array, while the Q outputs scan the bimorph drive array. As described above, the shift-register scan begins a short time after the leading edge of the bimorph drive waveform. The delay is determined by the clear delay circuit. The delay, Δ, is needed since the comparators are energized at the leading edge of the bimorph drive waveform, and a short settling time is necessary before scan initiation and the application of photo signals. Proper initiation of the scan, in spite of the asynchronism of the clocks, is the task of the pulse insertion flip-flop. It is set at the beginning of the bimorph drive waveform, and, in turn, sets the first shift-register stage when the clear delay is completed. After scan is initiated, feedback from the first shift-register stage resets the pulse insertion flip-flop and assures that one and only one pulse shifts through the register. After the last (24th) shift-register pulse, the comparators are de-energized. They remain de-energized for the remainder of the frame time, since no signal processing is required until the beginning of the next shift-register cycle. The ladder diagram, Fig. 14, shows the form of the various timing waveforms. Low-power RTL (MC700P) integrated circuits are used for the clocks, and low-power TTL (SN74L) for all of the logic. The low-power TTL was particularly useful because its active pull-up eliminated the need for any buffering of the shift register outputs.

The comparator circuit, illustrated in Fig. 15, is composed of a 709 operational amplifier followed by a RS flip-flop. It operates such that a dark element, i.e., a phototransistor output below threshold, energizes its corresponding simulator. To accomplish this, the scan clock resets the flip-flop at the beginning of each sample time into the appropriate (low output) state to turn on a bimorph drive transistor. However, if a phototransistor peak output exceeds threshold, the operational amplifier output overrides the scan clock reset, and sets the flip-flop in the "don't drive" condition. The venerable 709 has the right combination of speed and low input current to perform well as the voltage comparator in the system.

The automatic threshold circuit (ATC) is important in improving performance by freeing the reader from all adjustments as the reflectively of the reading material varies. The simple algorithm of setting the light or dark quantization threshold at a fraction, usually $\frac{1}{2}$, of the peak phototransistor signal in a column has proven quite effective. The ATC circuit, Fig. 16, consists of a resistive divider on one of the column load resistors, and a standard operational amplifier negative peak detector circuit. The ATC decay time constant, as dictated by resistor R and capacitor C, is chosen to be quite long—about 10 seconds. For this reason only one array column needs to be monitored, since the scanning causes all columns to be statistically identical.

Primary reading-aid power is supplied by four 1.25-volt size-D rechargeable nickel-cadmium batteries which

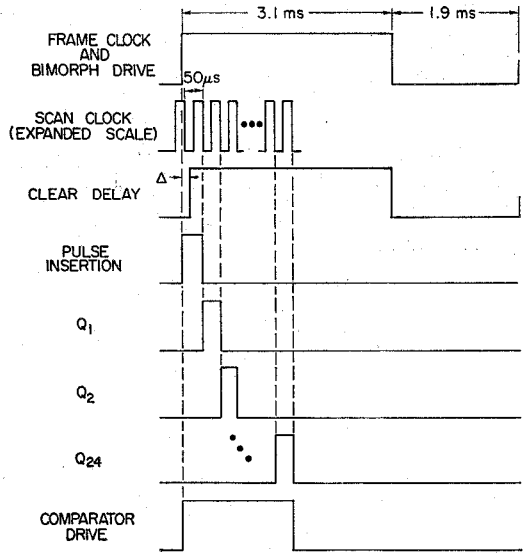

Fig. 14. Circuit waveforms.

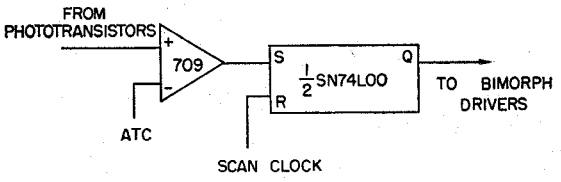

Fig. 15. Comparator circuit.

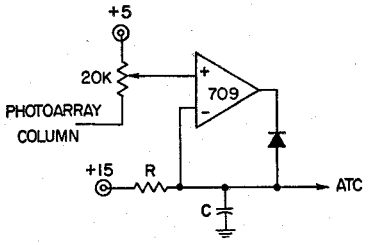

Fig. 16. ATC circuit.

provide the 5 volts required by most of the circuitry and the lamps. Two other supply voltages are needed, +15 volts for the operational amplifiers, and +30 volts for the stimulator drive (+60 volts for series-poled bimorphs). These voltages are generated by a highly efficient dc–dc converter. Power consumption of the total electronics, including all bimorphs, is under 0.5 watt. Including 1-watt for the page illumination, about 12 hours of battery-powered operation are possible without recharge.

The electronics are presently packaged beneath the tracking aid, as seen in Fig. 1. Future designs will incorporate a much more compact electronics package in conjunction with the stimulator array.

III. Conclusions

The feasibility of an optical-tactile reading aid based on the direct translation approach has been firmly established. Integrated electronics contribute directly to many of the singular features of the design, such as the integrated phototransistor sensing array that enables a small hand-held probe to be used, and the battery-powered, easily portable mutliplex electronics package. The output stimulator array, comprised of 144 vibratory piezoelectric bimorphs, is also a novel system feature. Three reading aids are presently in operation, and several more will be fabricated in the near future.

Work is continuing along many paths, including fundamental physical and psychophysical studies, integrated-circuit design, hardware design, and test and evaluation of reading performance. The latter is, of course, most crucial with respect to our ultimate goal. Reading speeds of 50 words per minute have been achieved with about 160 hours of practice, and ultimate limits have yet to be reached. Also, techniques for increasing the information processing capability of the reading aid are under scrutiny, in an attempt to greatly increase the possible reading rate. These techniques include increased field of view using either fixed or variable resolution, use of preprocessing character "clean-up," and use of a multilevel grey scale.

Many possible modes of operation for the reading aid, or similar cousins, in addition to that described are envisaged. These include input to a central computer facility with spoken output via phone lines, viewing of the environment, and the reading of printed braille. In its present form, it seems quite reasonable that the reading aid described in this paper could become widely used among the blind, and perhaps serve as a model for the application of contemporary technology to human problems.

Acknowledgment

The authors gratefully acknowledge the constant encouragement and advice of J. G. Linvill, the valuable suggestions of J. C. Bliss, and the helpful assistance of other members of the reading-aid project. Special recognition is due to J. Baer and J. Gill of Stanford Research Institute, who designed and fabricated the stimulator array and most of the probe hardware.

References

[1] V. K. Zworykin and L. E. Flory, "An electronic reading aid for the blind," *Proc. Am. Phil. Soc.*, vol. 91, pp. 139–142, 1947.
[2] J. S. Abma, "The Battelle aural reading device for the blind," in *Human Factors in Technology*, E. Bennett, J. Degan, and J. Spiegel, Eds. New York: McGraw-Hill, 1963, pp. 315–325.
[3] G. C. Smith, "The development of recognition and direct translation reading machines for the blind," *Proc. Internatl. Conf. on Sensory Devices for the Blind*, R. Dufton, Ed. Bristol: J. W. Arrowsmith, Ltd., 1967, pp. 367–388.
[4] E. E. Fournier d'Albe, "On a type-reading optophone," *Proc. Roy. Soc.*, vol. 90, pp. 373–375, May 1914.
[5] J. C. Bliss, "A relatively high-resolution reading aid for the blind," *IEEE Trans. Man-Machine Systems*, vol. MMS-10, pp. 1–9, March 1969.
[6] J. C. Bliss, M. H. Ketcher, C. H. Rogers, and R. Shepard, "Optical-to-tactile image conversion for the blind," presented at the Tactile Displays Conf., Stanford Research Institute, Menlo Park, Calif., April 1969 (to be published).
[7] J. G. Linvill and J. C. Bliss, "A direct-translation reading aid for the blind," *Proc. IEEE*, vol. 54, pp. 40–51, January 1966.

[8] R. C. Joy and J. G. Linvill, "Optoelectronic circuitry for a reading aid," *IEEE J. Solid-State Circuits*, vol. SC-3, pp. 451–453, December 1968.
[9] J. D. Meindl, J. D. Plummer, P. J. Salsbury, and J. S. Brugler, "Integrated electronics for a reading aid for the blind," *1969 ISSCC Digest Tech. Papers*, pp. 50–51.
[10] P. K. Weimer, W. S. Pike, G. Sadasiv, F. V. Shallcross, and L. Meray-Horvath, "Multielement self-scanned mosaic sensors," *IEEE Spectrum*, vol. 6, pp. 52–65, March 1969.
[11] P. J. Salsbury and J. D. Meindl. "A monolithic image sensing array for a reading aid for the blind" (to be published).
[12] G. P. Weckler, "Operation of *p-n* junction photodetectors in a photon flux integration mode," *IEEE J. Solid-State Circuits*, vol. SC-2, pp. 65–73, September 1967.
[13] R. C. Joy and J. G. Linvill, "Phototransistor operation in the charge storage mode," *IEEE Trans. Electron Devices*, vol. ED-15, pp. 237–248, April 1968.
[14] J. S. Brugler, "Low-light-level limitations of silicon junction photodetectors," Stanford Electronics Labs., Stanford, California, Rept. SU-SEL-68-041, TR No. 4824-1, May 1968.
[15] P. A. Gary and J. G. Linvill, "A planar silicon photosensor with an optimal spectral response for detecting printed material," *IEEE Trans. Electron Devices*, vol. ED-15, pp. 30–39, January 1968.

Sneak Paths in $X-Y$ Matrix Arrays

DANIEL C. OSBORN, MEMBER, IEEE

***Abstract*—In this paper, an equivalent circuit of an image sensor matrix is derived for a general array containing r rows and c columns. The circuit is useful in determining the "sneak paths" that exist, the amount of element isolation required, and/or the maximum array size possible for a given design. The various sneak paths that exist and general methods to minimize them are discussed. The matrix element employed is a photoconductor in series with a p-n junction diode. The circuit derivation is also applicable to the analysis of many photosensor arrays, with or without charge storage, as well as matrix display and memory arrays.**

Introduction

COMPUTER core memories and communication switching networks have used X–Y matrix address schemes extensively. Matrix addressing is desirable since the number of selection circuits are reduced compared to a direct connection to each element individually. Therefore, these schemes are also being applied to a number of large-scale microelectronic components; for example, solid-state image sensors, flat panel displays, and semiconductor memories.

In a matrix array with many semiconductor devices connected electrically across row and column conductors, the relatively high interelement signal isolation that is inherent in magnetic flux coupling and electromagnetic relays is not available. Signal coupling between adjacent conductors, and sneak paths through the matrix, are likely unless the necessary degree of isolation is provided.

A number of promising solid-state image array schemes have been reported in the literature [1]–[7]. However, no convenient method to analyze large arrays is known to have been reported. In this paper an equivalent circuit of an image sensor matrix is derived for a general array containing r rows and c columns. The circuit is useful in determining the sneak paths that exist, the amount of element isolation required, and/or the maximum array size possible for a given design. The equivalent circuit is useful even when a computer-aided analysis is performed, since computing considerations such as running time, storage requirements, and cost are substantially reduced. The circuit derivation is also sufficiently general as to be extendable to the analysis of many photosensor arrays with or without charge storage as well as matrix display and memory arrays.

The equivalent circuit was used in the design of an integrated image sensor array, utilizing a photoconductor–capacitor–diode charge storage element, and discrete transistor selection circuitry. This fabrication effort has been described in [1].

Sensor Array Operation

An X–Y matrix array is an assembly of a number of identical devices or groups of devices, hereafter called the matrix elements. Each element is located at the intersection of, and, is connected to, a single row and a single column of a row–column conductor matrix. Each element has at least two external terminals, and contains at least a photosensor and some form of isolation device. The photosensors are usually arranged in a planar mosaic and means are provided for imaging the optical input. The electrical parameter of the photosensor that is related to the incident illumination is determined by a readout or selection process. For example, a known voltage is applied to each element in sequence and the resulting current pulses are combined into a video signal. For clarity, the equivalent

Manuscript received April 15, 1969; revised June 16, 1969. Portions of this work were sponsored by the NASA Marshall Space Flight Center, Huntsville, Ala., under Contract NAS8-5116.
The author was with the Electronics Laboratory, General Electric Company, Syracuse, N. Y. He is now with Systems, Science and Software, La Jolla, Calif.